

CALCULATION OF ROTOR WORK ON THE BASIS OF THERMOANEMOMETRIC MEASUREMENT RESULTS. PART 2

SUMMARY

In the second part of the article the correction of the balance method has been made by reduction of parameters to those sections where measurements of airflow velocity and the work determination were done. As losses of energy in supply line rotor between measure section and inlet as well as losses of energy in consequence of slot bypass leakage were taken into consideration, both methods of measurements gave the same increases of energy in the rim of rotor. Therefore, the methods may be considered as equivalent. The methods of field velocities and turbulence coefficient averaging were analysed with the aim to develop optimal measurement conditions.

Keywords: losses energy on rotor, rotor work

PORÓWNANIE PRACY WIRNIKOWEJ WYZNACZONEJ NA PODSTAWIE WYNIKÓW POMIARÓW TERMOANEMOMETRYCZNYCH I BILANSOWYCH. CZĘŚĆ 2

W drugiej części artykułu dokonano korekcji metody bilansowej przez sprowadzenie zmierzonych parametrów do tych przekrojów, w których dokonano termoanemometrycznych pomiarów prędkości przepływu powietrza i określono pracę. Dzięki uwzględnieniu strat energii w przewodzie zasilającym wirnik pomiędzy przekrojem pomiarowym a wlotowym oraz strat energii na skutek przecieku bajpasowego na szczelinie stwierdzono, iż obie metody pomiarów dają takie same przyrosty energii w wieńcu wirnika. Są zatem równoważne. W celu opracowanie optymalnych warunków pomiaru przeanalizowano sposoby uśredniania pól prędkości oraz współczynnika turbulencji.

Słowa kluczowe: praca wirnikowa, straty energii w wirniku

1. INTRODUCTION

In the first part of the article velocities c_{2m} and c_{2u} measured with the thermoanemometer became the basis for five rotary velocities to calculate useful whirl work l_{u1-2} , which was compared with the useful work resulted for balance measurements l_{us-2} . The author aim is to verify both types of tests to appraise precision of thermoanemometric method and analyse its usability for general use in testing of radial fans.

Results of Part I are shown in Table 1.

The following concepts have been defined for the needs of analyses of results obtained with both methods:

– capacity difference $\Delta \dot{V}_s = \dot{V}_{sz} - \dot{V}_{sa}$ (1)

– work difference $\Delta l_u = l_{uz} - l_{ua} = l_{us2} - l_{u12}$ (2)

– relative capacity difference $\frac{\Delta \dot{V}_s}{\dot{V}_{sz}} = \delta_v \%$,

– relative work difference $\frac{|\Delta l_u|}{l_{u12}} = \delta_l \%$,

where:

\dot{V}_s – fan capacity measured in the fan suction pipe,

l_u – useful work,

indices:

z – values measured with a reducer in balance method,

a – values measured with thermoanemometer,

12 – values measured at the line between sections 1–2,

$s2$ – values measured at the line between sections s –2.

Relative differences δ_v and δ_l are shown in Table 2.

Table 1. List of capacity and work increase calculated on the basis of thermoanemometric measurements

It.	\dot{V}_{sz} , m/s	\dot{V}_s , m/s	$\Delta \dot{V}_s$, m/s	$l_{us2} = l_{uz}$, m ² /s ²	$l_{u12} = l_{ua}$, m ² /s ²	Δl_u , m ² /s ²
	1	2	3	4	5	6
1	0.0880	0.0670	+0.0210	19.2	23.8	–4.6
2	0.1350	0.1354	–0.0004	77.8	88.5	–10.7
3	0.2140	0.2043	+0.0097	181.0	203.6	–22.6
4	0.3220	0.3316	–0.0096	420.5	460.3	–39.8
5	0.3500	0.3460	+0.0040	507.0	612.3	–75.3

* AGH University of Science and Technology, Kraków

Table 2. Relative differences of capacity and work

It.	$\delta_v, \%$	$\delta_l, \%$
1	23.9	19.3
2	0.3	12.1
3	4.5	11.1
4	3.0	8.6
5	1.1	12.2

Uncertainty of thermoanemometric capacity measurements is not significantly different from uncertainty of reducer method. However, uncertainty of defining energy increase in the rotor is quite significant, though it corresponds to uncertainty of calculations of flow performance based on analytical methods. That is the reason why thermoanemometric methods are interesting and requires additional development of thermoanemometric experiment pragmatics which will allow precise enough measurements of flow parameters. Material contained in Part I allows us to notice that energy balance in the rotor was measured between $s-2$ sections, and energy increase defined on the basis of thermoanemometric measurements is determined between rim sections 1–2. Loss which differentiate both works occurs in pipeline between the sections (see Fig. 1). Therefore we should consider pressure loss in three elements between $s-2$ sections, that is straight axis pipe, where gas flows with velocity c_s , funnel and inlet chamber. Air direction is changed here, delays velocity from c_w to $c_{1m} = c_{1r}$ and is mixed with \dot{V}_r stream leaking through the slot. If we take losses into consideration, differences in work Δl_u shown in Table 1 (column 6) may be significantly reduced, because this part of the article deals with calculations of losses occurring at the length of $s-1$. The other reason of differences between both works may be energy loss connected with stream leakage from the slot. Slot stream losses energy earlier obtained from the rotor when it circulates round the front disk of the rotor. One of other reasons of inaccuracies

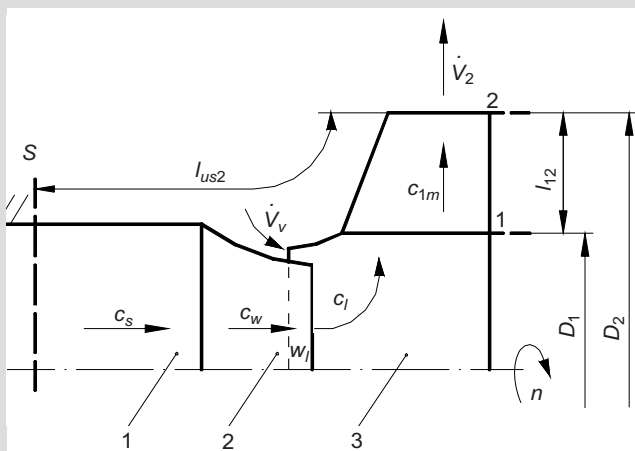


Fig. 1. Measure sections: section 1–2 for thermoanemometric measurements Velocities and section $s-2$ for energy balance calculations; 1 – pipe, 2 – funnel, 3 – rotor inlet chamber

in both balances may be the averaging method of velocities measured at the outlet section of the rotor. In this view, we shall analyse velocities in relation to time and rotor width, turbulence courses and sampling time of velocity readings

2. CORRECTION OF BALANCE MEASUREMENT RESULTS FOR 1–2 SECTION

Figure 1 depicts location of three sections at the radial stage, where total pressure is measured with thermoanemometer or balance method. Thermoanemometric measurements of components c_r , c_u , c_z and module c are made in section 2 behind the rotor. Radial component c_r allows measurement of rim capacity, and peripheral component c_u allows measurement of energy increase in the rotor, because component $c_{1u} = 0$ is located in section 1 according to the assumed irrotational flow.

Energy is transmitted to the medium between sections 1 and 2. It may be calculated on the basis of the measured peripheral velocity c_{2u} .

Balance results determined between $s-2$ sections should be referred to 1–2 section, taking into account energy losses occurring during the flow from section s to section 1. Energy losses occur on the way between sections due to friction in the pipe, funnel, and rotor inlet chamber. These losses cause energy drop in section 1 equal to the total of losses in the specified elements, as expressed by the equation

$$l_{us2} + l_{u1} + l_{u2} + l_{u3} = l_{u12} \quad (4)$$

where:

- l_{us2} – energy increase between $s-2$ sections, determined according to balance measurements,
- l_{u1} – energy loss in pipe,
- l_{u2} – energy loss in funnel,
- l_{u3} – energy loss in rotor inlet chamber,
- l_{u12} – energy transmitted to the medium in the rotating rotor, determined with thermoanemometric measurements.

Experiment described in literature [6] was made in order to determine losses $l_{u1,2,3}$. The experiment allows determination of energy loss with $\xi_{1,2,3}$ coefficient referred to velocity in suction pipe c_s , according to the formula

$$l_{u1,2,3} = \xi_{1,2,3} \frac{c_s^2}{2} \quad (5)$$

where:

$$c_s = \frac{\dot{V}_{sz}}{A_s} = 26.32 \dot{V}_{sz},$$

A_s – inlet section area.

Energy loss coefficient was determined for a set of three elements supplying the rotor. Separation of elementary loss would not be correct because of interaction of these elements and, as it is necessary to preserve correct energy measurement conditions.

Table 3. List of energy losses in three-element fitting and measurement uncertainty after correction of losses

It.	c_s , m/s	$\xi_{1,2,3}$, m^2/s^2	$l_{u1,2,3}$, m^2/s^2	$l_{us2} + l_{u1,2,3} = l_{u12z}$, m^2/s^2	$l_{u12} = l_u$, m^2/s^2	Δl_u , m^2/s^2	δ_1 , m^2/s^2
	1	2	3	4	5	6	7
1	2.32		2.2	21.4	23.8	-2.4	10.0
2	3.50		5.1	82.9	88.5	-5.6	6.7
3	5.63	0.83	13.1	194.1	203.6	-9.5	4.9
4	8.47		29.8	450.3	460.3	-10.0	2.2
5	9.20		35.2	572.2	612.3	-40.1	7.0

Results of energy loss calculations are shown on Table 3.

Value of energy losses in rotor supply between measurement section and rim l_{us1} inlet of the tested fan was about 6% (9.2; 5.7; 6.4; 6.4; 5.7 subsequently for intervals 1 to 5) of the energy transmitted to the medium. This value of losses was obtained from the ratio of values in column 3 to values of column 5.

Having considered the losses, it appears that work values defined with the balance method and shown in column 4 are only slightly different from work values measured with thermoanemometer and shown in column 5. This slight difference at the level not exceeding 10% at l_{u12} is caused with the energy loss in volumetric leakage.

3. CORRECTION OF WHIRL WORK BECAUSE OF VOLUMETRIC LOSS

Energy balance made for sections s and 2 refers to other streams of the volume resulted from volumetric leakage. Capacity of \dot{V}_s fan is determined in section s , and \dot{V}_2 capacity determined in section 2 is enlarged with \dot{V}_v slot stream. The stream leaking through the slot recirculates round the front disk of the rotor at the cost of energy obtained in the rotor. This part of energy connected with the volumetric stream is irreparably lost when gas returns to the inlet chamber instead of operating in the useful stream. This energy loss l_v should be added to the energy balance of suction stream \dot{V}_s , that is, we obtain

$$l_{us2} + l_{u1,2,3} + l_v = l_{u12} \quad (6)$$

Then, energy which as been experimentally determined with the balance method will be equal to energy determined with thermoanemometer

$$l_{uz} \approx l_{ua} \quad (7)$$

Energy losses originating from non-linear loss may be calculated:

$$l_v = \frac{\dot{V}_v}{V_2} \cdot l_{ua} \quad (8)$$

Results of l_v losses calculations are shown in Table 4.

When energy loss resulted from volumetric leakage have been taken into consideration, deviation δ_1 is reduced. Therefore, the deviation between results δ_1 in column 6 Table 4 refer to values other than zero.

It should be noted, however, that conformity of results in both measurements is sufficient, and both measurements may be treated as equal testing methods.

4. FURTHER RESULTS OF THERMOANEMOMETRIC MEASUREMENTS

Courses of velocity components c_m , c_u , c_z , and module c in the rotor rotating with velocity of 2260 r.p.m. are shown in Figures 2 and 3. The first top record refers to measurements with the sensor located just next to the rotor carrying disk.

Table 4. Energy losses in slot duct

It.	\dot{V}_s , m^3/s	\dot{V}_2 , m^3/s	l_{ua} , m^2/s^2	l_v , m^2/s^2	$l_{u12z} + l_z = l_{u12}$, m^2/s^2	δ_1 , %
	1	2	3	4	5	6
1	0.0050	0.0721	23.8	1.65	23.05	3.1
2	0.0102	0.1456	88.5	6.20	89.10	0.6
3	0.0155	0.2202	203.6	14.33	208.43	2.4
4	0.0250	0.3566	460.3	32.27	482.57	4.8
5	0.0254	0.3720	612.3	41.80	614.00	0.3

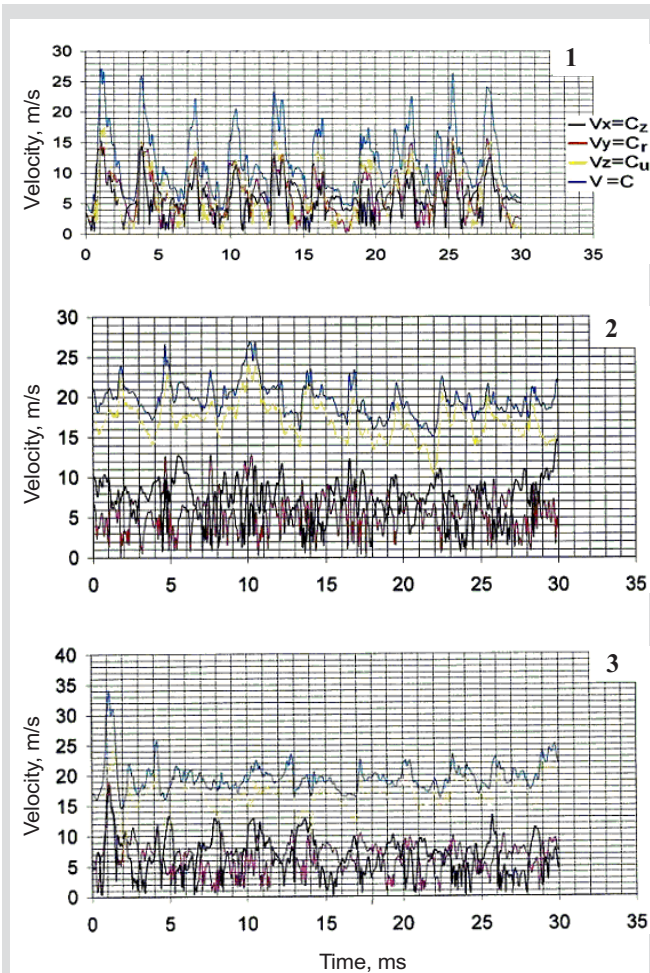


Fig. 2. Time courses of velocities c , c_u , c_r , c_z measured in the vicinity of the carrying disk (1) and in the distance of $b = 14$ (2) and 28 (3) mm from the disk

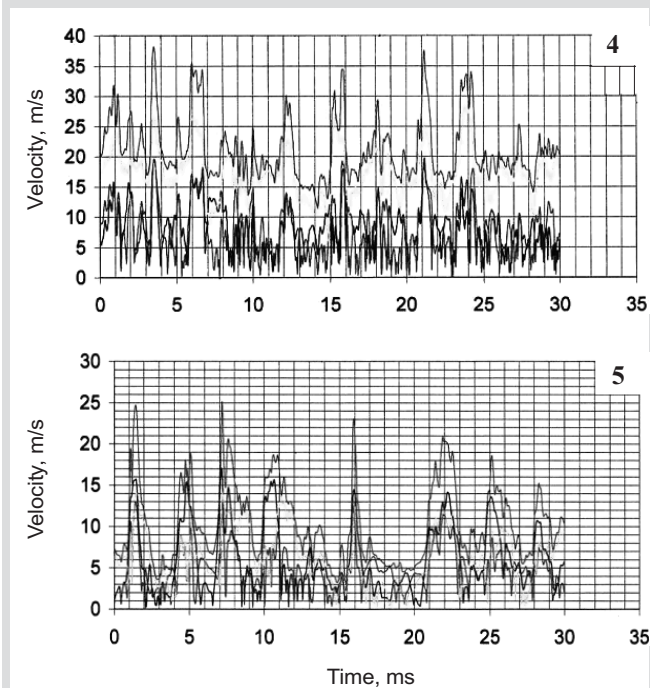


Fig. 3. Time courses of velocities c , c_u , c_r , c_z measured in the distance of 42 mm (4) from the carrying disk and in the vicinity of the front disk (5)

Next diagrams are made with the sensor located 14 mm (2) from the back disk, the next diagram (3) was made at the half of the rotor width, that is 28 mm (3) from the back disk. The next figure (3) shows records of two sensor positions – 42 and 56 mm from the back disk. The smallest amplitudes of all velocities are at the half of the rotor width.

The time courses were used to calculate average values in the function of blade width and rotary speed. These results are shown in Table 5 and Figure 2, part 1. Manner of averaging the velocity along the blade width affects the obtained results. Scale of sensor positioning has the same effect. If a sensor is placed every 2 mm, average values are $c_r = 6.69$ m/s, $c_u = 15.48$ m/s. When it is placed every 4 mm from the back disk, the average value of components is $c_r = 6.60$ m/s, $c_u = 15.40$ m/s. Four uniform positioning along the blade width will allow to calculate values $c_r = 6.58$ m/s i $c_u = 15.42$ m/s. Averaging in time function is performed with frequency of 5 kHz. Manner of averaging affects the obtained measurement results.

Table 5 shows time averaging velocity components for various sensor positions and average value obtained from time averages.

Figure 4 shows results of turbulence tests for a rotor wheel rotating with 5 speeds.

Average values of turbulence coefficient are shown in Table 6.

The coefficient Turb y and z is defined

$$\sigma_T = \frac{\sqrt{\sum_{i=1}^n (V_i - \bar{V})^2}}{n\bar{V}},$$

where:

- n – number of samples,
- V_i – spot speed of gas,
- \bar{V} – average speed of gas.

Turbulence coefficients reach high values for radial and axial velocities and low values for speed module and peripheral component.

5. SUMMARY

The analysis of anemometric and balance measurements of energy allows to state that both methods are equal with regard to the obtained measurement precision. Thermoanemometric measurement requires experience and great knowledge. This method is relatively cheap and may be the basic method for measuring air flow velocity. The advantages of the method are: point measurement, lack of moving elements disturbing the measured field, electric output signal easily automates the method. The drawback of the method is dependency of precision on velocity, temperature and chemical composition of gas.

The performed comparative measurements allowed to determine optimal conditions for application of the thermoanemometric method.

Table 5. List of velocities averaging against the time, and determined with thermoanemometer for 1–5 measurements in function of sensor positioning

Measurement 1						Measurement 2					
	mm	$V_x = c_z$	$V_y = c_r$	$V_z = c_u$	$V = c$		mm	V_x	V_y	V_z	V
H0010	0	1.1893	1.2352	1.3709	2.3349	H0020	0	2.2518	2.3051	2.3518	4.1675
H0610	6	1.4671	1.1777	2.2774	3.1175	H0620	6	2.8623	3.0435	5.8655	7.4808
H1110	11	1.709	1.2092	3.0564	3.8216	H1120	11	2.8185	2.7324	6.6626	7.9888
H1710	17	1.5948	1.1892	3.5525	4.1599	H1720	17	2.5367	2.4256	7.2374	8.1831
H2210	22	1.2763	1.1644	3.5204	3.9928	H2220	22	2.5059	2.5482	7.0516	8.0267
H2810	28	1.3227	1.1978	3.7656	4.2343	H2820	28	2.6485	2.7508	7.2925	8.3577
H3310	33	1.334	1.4127	3.6406	4.2156	H3320	33	2.5199	2.9204	7.2757	8.3547
H3910	39	1.3942	1.5796	3.5039	4.1815	H3920	39	2.6338	3.2269	7.2218	8.4861
H4410	44	1.5338	1.6577	3.1971	4.0515	H4420	44	2.7055	2.9733	5.694	7.2355
H5010	50	1.3468	1.2235	2.2444	3.0148	H5020	50	2.7611	2.419	3.7711	5.5716
H5510	55	1.3861	1.1866	1.2912	2.3631	H5520	55	1.6429	1.4186	1.503	2.7679
10	average	1.414	1.294	2.8564	3.5898	20	average	2.5352	2.6149	5.6297	6.9655
Measurement 3						Measurement 4					
	mm	V_x	V_y	V_z	V		mm	V_x	V_y	V_z	V
H0030	0	3.8668	4.1647	4.4586	7.591	H0045	0	4.2168	4.848	4.7702	8.3941
H0630	6	4.1486	4.297	7.5904	10.1201	H0645	6	5.8192	6.5133	9.2089	13.3431
H1130	11	3.9355	3.8543	9.5544	11.3799	H1145	11	5.4537	6.4999	13.744	16.6118
H1730	17	3.4446	3.4631	10.5313	11.7934	H1745	17	4.835	6.0949	15.2173	17.3586
H2230	22	3.5212	3.6529	10.3996	11.7488	H2245	22	4.7317	6.322	15.4868	17.5936
H2830	28	3.5729	4.0001	10.5809	12.0309	H2845	28	5.2982	6.2892	15.7349	17.9795
H3330	33	3.5576	2.287	10.5174	12.0862	H3345	33	5.7101	6.9133	15.649	18.2631
H3930	39	3.5948	4.545	10.3634	12.0647	H3945	39	5.5596	7.1728	15.1298	17.8676
H4430	44	3.6887	4.5498	9.5457	11.4629	H4445	44	5.4951	7.4292	13.7002	16.8787
H5030	50	3.7903	3.9802	6.6999	9.0688	H5045	50	5.6047	6.1194	10.2131	13.7239
H5530	55	3.3789	2.694	3.4671	5.8498	45	average	5.2724	6.4202	12.8854	15.8014
30	average	3.682	3.9535	8.519	10.4724						
Measurement 5											
	mm	V_x	V_y	V_z	V	Hs2850	28	6.4485	6.399	16.7719	19.4594
Hs0050	0	5.7944	6.3147	6.4688	11.1806	Hs3050	30	6.2206	6.5014	16.9104	19.5137
Hs0250	2	7.051	8.5219	12.4854	17.4831	Hs3250	32	6.2409	6.372	16.9066	19.4644
Hs0450	4	7.6084	8.0068	15.0652	19.3578	Hs3450	34	6.6318	6.9865	16.9549	19.8831
Hs0650	6	8.4244	6.5432	16.5548	20.2176	Hs3650	36	6.9557	7.205	16.9114	20.0978
Hs0850	8	8.1508	5.7411	15.9576	19.1392	Hs3850	38	7.2234	7.258	17.2495	20.5089
Hs1050	10	8.0291	5.3065	17.1638	19.9817	Hs4050	40	7.3968	7.6262	17.9054	21.2439
Hs1250	12	7.6897	5.3839	17.026	19.7739	Hs4250	42	8.2589	8.3721	17.5595	21.6563
Hs1450	14	7.0931	5.8563	16.8183	19.4797	Hs4450	44	7.1937	7.8317	17.2165	20.6842
Hs1650	16	7.036	5.9122	16.8414	19.54	Hs4650	46	7.381	7.6991	16.9737	20.5678
Hs1850	18	6.8146	6.2042	17.1414	19.8278	Hs4850	48	7.0744	7.5172	16.4524	19.9431
Hs2050	20	7.1347	6.278	16.0824	19.0404	Hs5050	50	7.6421	6.9195	14.7144	18.5922
Hs2250	22	6.1502	6.2359	16.9763	19.3877	Hs5250	52	8.1451	6.6516	12.0708	16.7201
Hs2450	24	6.5221	6.6113	16.6796	19.4568	Hs5450	54	8.388	6.15	9.4831	14.6893
Hs2650	26	6.2871	6.5797	17.1029	19.6962	Hs5650	56	6.4481	5.0209	6.4883	10.9153
						50	average	7.15292	6.68996	15.48044	18.87937

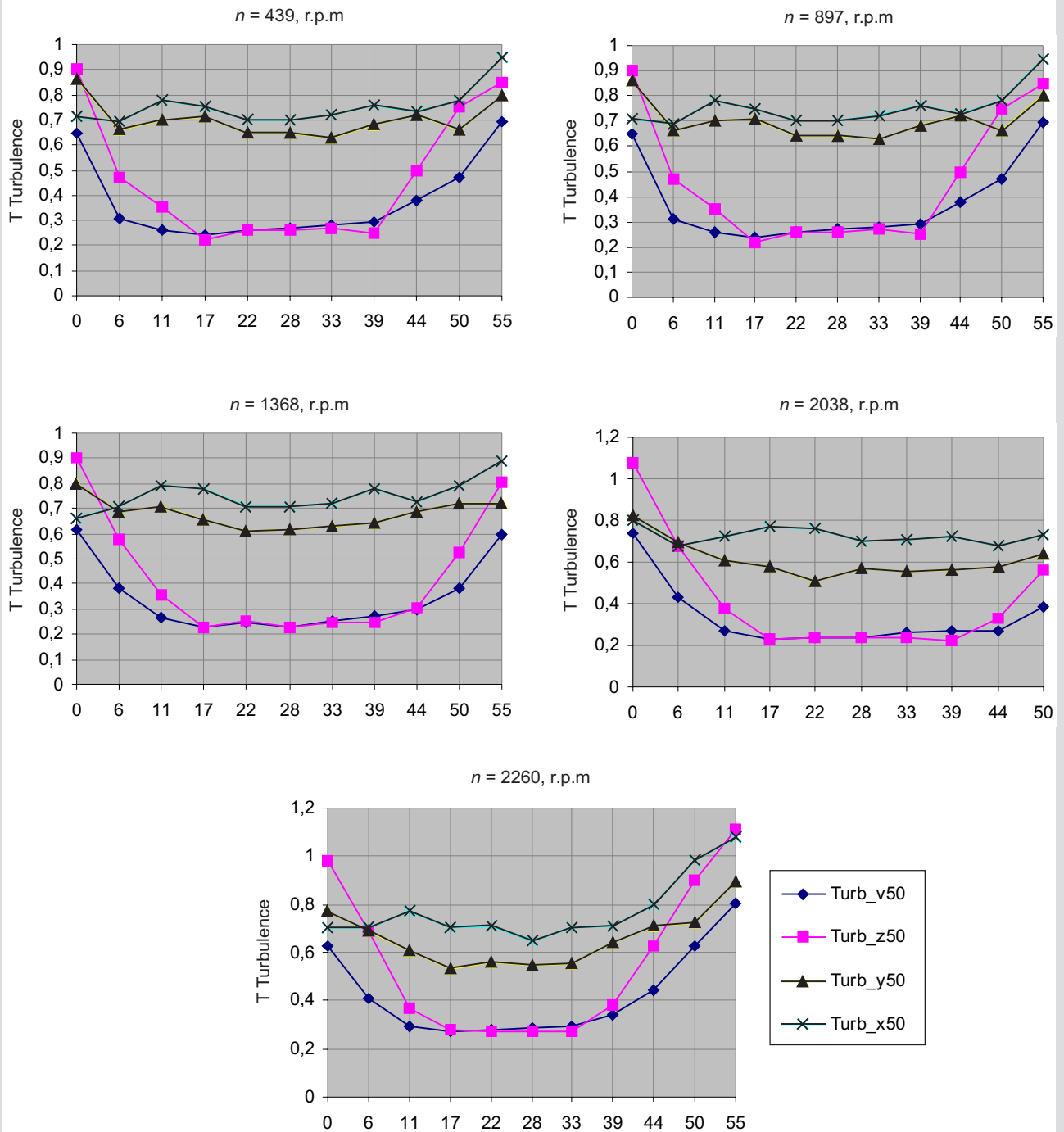


Fig. 4. Turbulence depending on distance from the back disk, for various rotations and components

Table 6. Average coefficient of radial and peripheral velocity components

It.	Revolutions, r.p.m	Turb_y (c_r)	Turb_z (c_u)
1	439	0.765	0.468
2	897	0.700	0.461
3	1368	0.680	0.425
4	2038	0.612	0.419
5	2260	0.656	0.558

Literature

- [1] Fortuna S. i in.: *Badania prędkości i poziomu turbulencji w strugach powietrza wypływających z koła promieniowego do swobodnej oraz ograniczonej przestrzeni*. Kraków, 2003 (praca niepublikowana)
- [2] Poleszczyk E.: *Termoanemometryczna metoda wyznaczania prędkości przepływu gazu*. Prace Instytutu Mechaniki Górotworu PAN, Kraków, 2002
- [3] Ligęza P.: *Pomiary termoanemometryczne w przepływach nieizotermicznych*. Pomiary, Automatyka, Kontrola, 1995
- [4] Gumuła S., Prync-Skotniczny K., Fortuna S.: *Prędkość i turbulencja przepływu powietrza w otoczeniu kół łopatkowych wentylatorów promieniowych*. Materiały VIII Międzynarodowej Konferencji „Przepływowe Maszyny Wirnikowe”, Politechnika Rzeszowska, Rzeszów, 1998
- [5] PN-76/M-34034: *Zasady obliczania strat ciśnienia*
- [6] Fortuna S.: *Wyznaczanie współczynnika strat w wybranych elementach wentylatora promieniowego*. *Ciepne maszyny przepływowe*. Turbomachinery, No. 126, Pol. Łódzka 2004